

Artificial Muscles Based on Ultra-Small Single-Walled Carbon Nanotubes

Vuong Van Thanh^{1*}, Nguyen Tuan Hung², Do Van Truong¹

¹ Hanoi University of Science and Technology – No. 1, Dai Co Viet Str., Hai Ba Trung, Ha Noi, Viet Nam

² Department of Physics, Tohoku University, Sendai 980-8578, Japan

Received: September 22, 2018; Accepted: June 24, 2019

Abstract

The effects of charge doping on the strain and electronic structure of ultra-small single-walled carbon nanotubes (SWNTs) are investigated by using first principle calculations. The obtained results show that the actuator strain and Fermi energy of the SWNTs are a function of charge doping level. The strain of the (2, 2) SWNT is larger than that of the (3, 3) SWNT at the same doping level due to their very large curvature effect. The strain of the (2, 2) SWNT obtained by charge doping ranging from -2.12% to 1.43%, which shows a candidate for the artificial muscle's application. In addition, the band structures of the SWNTs at the neutral and charge doping cases are also discussed in this present study.

Keywords: Ab initio, Carbon nanotubes, Artificial muscle, Density functional theory

1. Introduction

One-dimensional (1D) carbon nanotubes have attracted for artificial muscles by scientists because their outstanding properties such as high strength, high stiffness and they can reversibly contract and expand in volume under an applied voltage, which is like a natural muscle [1-3]. Baughman *et al.* [4, 5] had built an artificial muscle based on the single-walled carbon nanotubes (SWNTs). By charge doping, this artificial muscle could generate force per unit area of about 26 MPa, which is approximately 100 times larger than that of natural muscle [6]. Recently, Hung *et al.* [7] investigated the electrochemical actuation of the (6, 6) armchair carbon nanotube bundles using the first principle calculations. They reported that the mechanical and electronic properties of the SWNTs bundles as a function of charge doping, in which the SWNTs bundles shows the large deformation under hole doping case. In addition, the changes of electronic properties in the individual SWNTs under charge doping have been investigated in previous studies [8, 9]. Although the SWNTs with large diameters are well known in the artificial muscles, the SWNTs with ultra-small diameter (0.3~0.4 nm) have an interesting mechanical property comparable to the SWNTs with large diameters.

For the ultra-small SWNTs, experimentally, the smallest stable (2, 2) SWNT with a diameter of 0.3 nm observed by Zhao *et al.* [10]. Theoretically, by using *Ab initio* first principle calculations, Hung *et al.* [11] studied the mechanical properties of SWNTs

under the uniaxial strain. They showed that the strength of ultra-small SWNTs is significantly reduced with the decreasing the tube diameter. In particular, the Young's modulus is significantly reduced in the ultra-small SWNTs with the diameter less than 0.4 nm due to their very large curvature effect. However, the electromechanical properties of ultra-small SWNTs under charge doping have not been clarified yet.

In this paper, the electromechanical properties of small armchair SWNTs with diameter of about 0.3 and 0.4 nm under charge doping are investigated by *Ab initio* density functional theory (DFT) calculations. Our results show the strain and Fermi energy of SWNTs as a function of charge doping. The Fermi energy of SWNTs decreases when increasing the charge doping level. Furthermore, the band structures of SWNTs are also investigated under charge doping.

2. Methodology

First-principles (*Ab initio*) calculations for the charge doping of the ultra-small SWNTs are performed by using Quantum-ESPRESSO (QE) package [12], which is a full density functional theory (DFT) simulations package using a plane-wave basis set [13, 14]. The Rabe-Rappe-Kaxiras-Joannopoulos (RRKJ) [15] ultrasoft pseudopotential is used to calculate the pseudopotential plane-wave with an energy cutoff of 60 Ry for the wave function. The exchange–correlation energy is evaluated by general-gradient approximation (GGA) [16] using the Perdew-Burke-Ernzerhof (PBE) [17] function.

In Fig. 1, we show the simulation models of the SWNTs including the armchair type (2, 2) and (3, 3), which have the diameters of about 0.3 and 0.4 nm.

* Corresponding author: Tel.: (+84) 947.288.086
Email: thanh.vuongvan@hust.edu.vn

Since a periodic boundary condition is applied for three dimensions in all models, the thickness of the vacuum region is set at 12 Å perpendicular to the tube axis to avoid the undesirable interactions from the neighboring SWNTs. The \mathbf{k} -point grids in the Brillouin zone selected according to the Monkhorst-Pack method is 1 x 1 x 12, where \mathbf{k} is the electron wave vector [18].

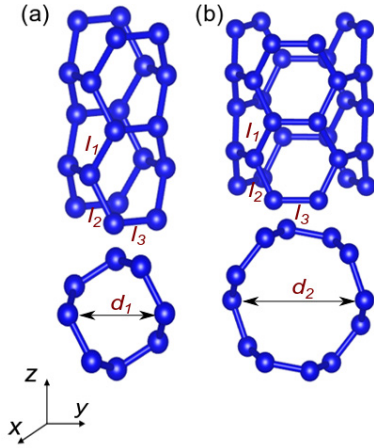


Fig. 1. The simulation models of (a) (2, 2) and (b) (3, 3) SWNTs. The notations of l_1 to l_3 are three bond lengths around C atom and d_1 and d_2 are diameters of the (2, 2) and (3, 3) SWNTs, respectively.

To investigate the effect of the charge doping on actuator strain and electronic properties of the SWNTs, the models are relaxed by using the Broyden-Fletcher Goldfarb-Shanno (BFGS) minimization method for the atomic positions, and cell dimensions in the z direction. These models are considered equilibrium until all the Hellmann-Feynman forces and the normal component of the stress σ_{zz} less than 5.0×10^{-4} Ry/a.u. and 1.0×10^{-2} GPa, respectively. To discuss the electromechanical actuation of SWNTs, the geometry optimizations are performed for each charge doping from -0.1 to +0.1 electron per atom (e/atom), in which the electron (hole) doping is simulated by adding (removing) electrons to the unit cell.

To calculate the strain of SWNTs as a function of the Fermi energy, the relative shift of the Fermi energy, ΔE_F , for the charge doping is defined as [7]

$$\Delta E_F = E_F^{\text{neutral}} - E_F^{\text{doped}} \quad (1)$$

where E_F^{neutral} and E_F^{doped} are the Fermi energy for the neutral and charge doping, respectively. The Fermi energy is defined by the center of the energy gap for the semiconducting SWNTs case. In the metallic SWNTs case, the Fermi energy is defined as the highest energy for occupied electrons.

3. Results and discussions

In order to study the variation of the structural deformation of the armchair SWNTs as a function of charge (electron and hole) doping, we define the strain along z direction as

$$\varepsilon_z = \Delta z / z_0 \quad (2)$$

where z_0 is the length c of the SWNTs in the unit cell at geometry optimization for neutral case and Δz is the increment of the length Δc under the charge doping level. The length c of the (2, 2) and (3, 3) SWNTs are 0.25 and 0.24 nm, respectively. As shown in Fig. 2, the strain ε_z of the (2, 2) and (3, 3) armchair SWNTs as function of the charge doping q ranging from -0.1 to +0.1 e/atom . In the neutral case ($q = 0$), we obtain $\varepsilon_z = 0$. For the charge (electron and hole) doping case, ε_z is a non-linear function of q . For the electron doping ($q < 0$), ε_z of the armchair SWNTs increase with decreasing of q . At $q = -0.1 e/\text{atom}$, the strains of the (2, 2) and (3, 3) armchair SWNTs are up to 1.34% and 0.59%, respectively. For the hole doping ($q > 0$), the (2, 2) SWNT shows an axial compression with the strain of about -2.12% at $q = 0.1 e/\text{atom}$, while the (3, 3) SWNT shows the highest compression strain ($\varepsilon_z = -0.17\%$) at $q = +0.04 e/\text{atom}$ and the expansion strain about $\varepsilon_z = 0.48\%$ at $q = +0.1 e/\text{atom}$. The results obtained show that the strain magnitude of the (2, 2) SWNT is higher than that of (3, 3) SWNT at the same charge doping level, which are dominated by their large curvature effect [11]. For the SWNTs and graphite, previous studies showed that the axial strain of SWNTs and graphite of about 1% can be achieved for both heavy electron and hole doping cases [19, 20]. In this present study, the strain magnitude of (2, 2) armchair SWNTs ranging from -2.12% to 1.43% by electron and hole doping, respectively, indicating that the electromechanical actuators of the utral-small SWNTs is better than that of the SWNTs with large diameters.

To understand the different strain of the SWNTs under the charge doping, we show the C-C bond lengths of the SWNTs as a function of charge doping in Fig. 3. We find that $l_1 = l_2$ for both the (2, 2) and (3, 3) SWNTs and the C-C bond lengths of the (2, 2) SWNT change larger than that of the (3, 3) SWNT at the same charge doping level. For the neutral case ($q = 0$), $l_{1,2}$ and l_3 of the (2, 2) SWNT are 1.490 Å and 1.391 Å, respectively, while $l_{1,2}$ and l_3 of the (3, 3) SWNT are 1.431 Å and 1.437 Å, respectively. For the hole doping ($q > 0$), $l_{1,2}$ and l_3 of the (2, 2) SWNT decreases and increases, respectively, with increasing of q . On the other hand, $l_{1,2}$ and l_3 of the (3, 3) SWNT increases and decreases, respectively, with increasing

of q . For electron doping ($q < 0$), $l_{1,2}$ of the (2, 2) SWNT is increased by 1.19% while l_3 is slightly decreased by 0.27% at $q = -0.1$ e/atom. In contrast, $l_{1,2}$ and l_3 of the (3, 3) SWNT are increased up to 0.49% and 0.34% at $q = -0.1$ e/atom, respectively. From the change of the C-C bond lengths under the charge doping, we can point out that the strain of (2, 2) SWNT is larger than that of (3, 3) SWNT at the same of q , as show in Fig. 2.

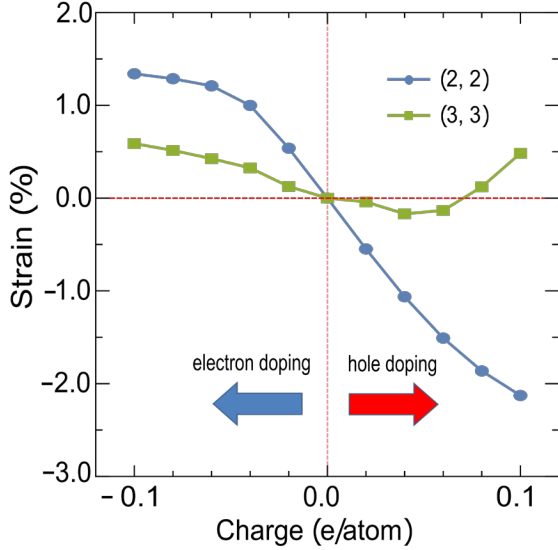


Fig. 2. Actuator strain of the (2, 2) and (3, 3) SWNTs as a function of charge doping.

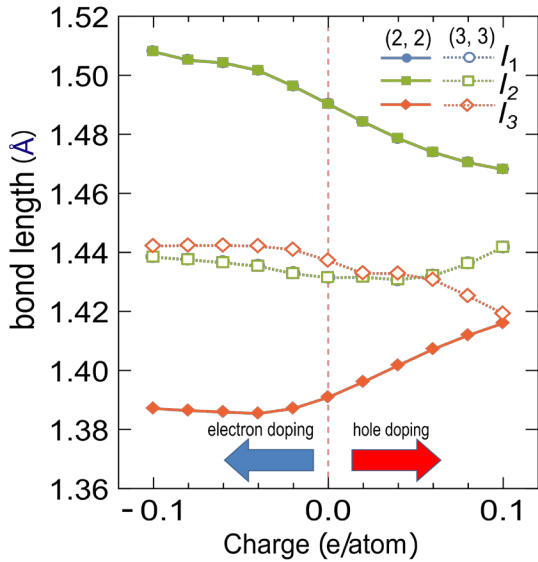


Fig. 3. C-C bond lengths l_1 , l_2 , l_3 of the (2, 2) and (3, 3) SWNTs as a function of charge doping.

In Fig. 4, we show ΔE_F as a function of q based on Eq. (1). In the neutral case ($q = 0$), $\Delta E_F = 0$ from

the definition in Eq.(1), while for the electron (hole) doping, ΔE_F monotonically decreases with increasing of q . $\Delta E_F > 0$ and < 0 for the electron and hole doping cases, respectively, because of the band structures of the SWNTs are changed by charge doping, as shown in Fig. 5.

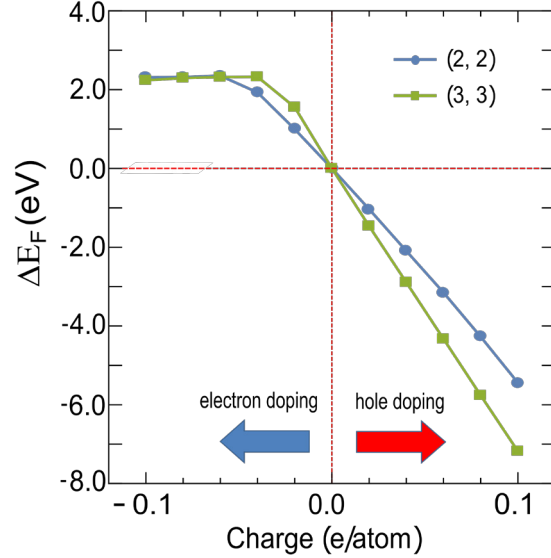


Fig. 4. ΔE_F as a function of q for charge doping.

To study the variation of the electronic properties of SWNTs under charge doping, we calculate the energy band structures of the (2, 2) and (3, 3) SWNTs for the neutral ($q = 0$), electron doping ($q = -0.1$ e/atom) and hole doping ($q = +0.1$ e/atom) cases. In Fig. 5(a) and (b), we show the band structures of (2, 2) and (3, 3) SWNTs, respectively. The dashed line shows the Fermi energy level. The obtained results show that (2, 2) SWNT is metallic for both the neutral case and charge doping, while (3, 3) SWNT is semi-metallic. For the electron doping case, the energy bands of SWNTs shift downward compared with the energy bands in the neutral case, which gives $\Delta E_F > 0$. On the other hand, for the hope doping case, the energy bands of SWNTs shift upward by increasing q , resulting in $\Delta E_F < 0$. As shown in Fig. 5(b), the Dirac energy point of the (3, 3) SWNTs is near the Fermi energy level at the neutral case. For the hole doping at $q = +0.1$ e/atom, the Dirac energy point moves upward, which is a good agreement with the (6, 6) armchair SWNT bundle [7]. On the other hand, the Dirac energy point moves downward at $q = -0.1$ e/atom for the electron doping.

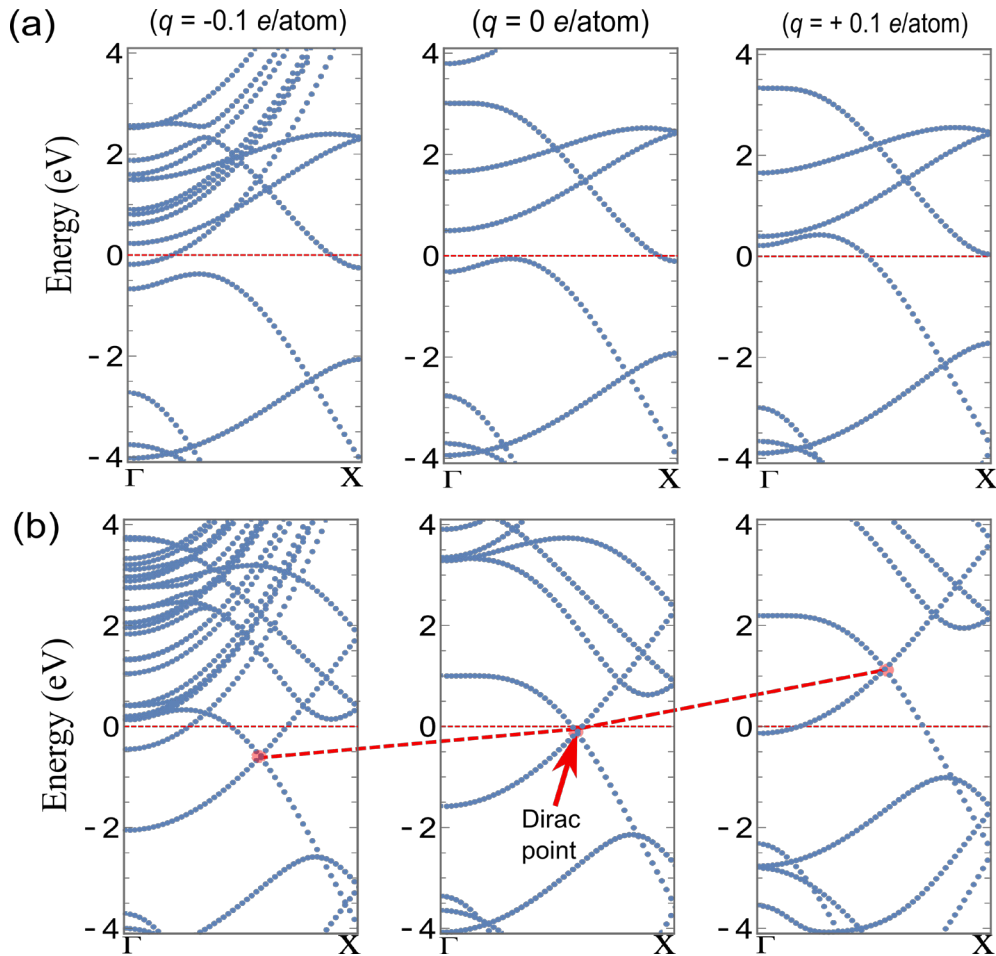


Fig. 5. Energy band structures of (a) (2, 2) and (b) (3, 3) armchair SWNTs with electron doping ($q = -0.1$ e/atom), neutral condition ($q = 0$ e/atom) and hole doping ($q = +0.1$ e/atom) cases. The Fermi energy (dashed line) is set to zero for all plots.

4. Conclusion

We have performed a first principles theoretical study on the electromechanical properties as a function of charge doping for the ultra-small (2, 2) and (3, 3) SWNTs. The study results can be summarized as follows:

- By charge doping, the electromechanical properties of the (2, 2) SWNT are better than that of the (3, 3) SWNT. In which, the (2, 2) SWNT shows a reversibly strain ranging from -2.12% to 1.34%, which is higher than SWNT with large diameter. Therefore, the (2, 2) SWNT is good candidate for artificial muscles.

- The Fermi energy of SWNTs depend on the charge doping level, which is decreased with increasing of the charge doping level.

- The (2, 2) SWNT is metallic, while the (3, 3) SWNT is semi-metallic at the neutral and charge doping cases.

Acknowledgments

This research is funded by the Hanoi University of Science and Technology (HUST) under project number T2017-LN-10.

References

- [1] M.F. Yu, O. Lourie, M.J. Dyer, K. Moloni, T.F. Kelly, R.S. Ruoff; Strength and breaking mechanism of multiwalled carbon nanotubes under tensile load; *Science* 287 (2000) 637–640.
- [2] M.F. Yu, B.S. Files, S. Arepalli, R.S. Ruoff; Tensile loading of ropes of single wall carbon nanotubes and their mechanical properties; *Phys. Rev. Lett.* 84 (2000) 5552.
- [3] H. Liu, D. Nishide, T. Tanaka, H. Kataura; Large-scale single-chirality separation of single-wall carbon nanotubes by simple gel chromatography; *Nat. Commun.* 2 (2011) 309.
- [4] R.H. Baughman, C. Cui, A.A. Zakhidov, Z. Iqbal, J.N. Barisci, G.M. Spinks, G.G. Wallace, A.

- Mazzoldi, D. De Rossi, A.G. Rinzler, O. Jaschinski, S. Roth, M. Kertesz; Carbon nanotube actuators; *Science* 284 (1999) 1340–1344.
- [5] R.H. Baughman, A.A. Zakhidov, W.A. de Heer; Carbon nanotubes—the route toward applications; *Science* 297 (2002) 787–792.
- [6] J.D.W. Madden, N.A. Vandesteeg, P.A. Anquetil, P.G.A. Madden, A. Takshi, R.Z. Pytel, S.R. Lafontaine, P.A. Wieringa, I.W. Hunter; Artificial muscle technology: physical principles and naval prospects; *IEEE J. Ocean. Eng.* 29 (2004) 706–728.
- [7] N.T. Hung, A.R. Nugraha, & R. Saito; Charge-induced electrochemical actuation of armchair carbon nanotube bundles; *Carbon* 118 (2017) 278–284.
- [8] L.C. Yin, H.M. Cheng, R. Saito, M.S. Dresselhaus; Fermi level dependent optical transition energy in metallic single-walled carbon nanotubes; *Carbon* 49 (2011) 4774–4780.
- [9] C. Li, T.W. Chou; Theoretical studies on the charge-induced failure of single-walled carbon nanotubes; *Carbon* 45 (2007) 922–930.
- [10] X. Zhao, Y. Liu, S. Inoue, T. Suzuki, R.O. Jones, Y. Ando; Smallest carbon nanotube is 3 Å in diameter; *Physical review letters*, 92 (12), (2004), 125502.
- [11] N.T. Hung, D.V. Truong, V.V. Thanh, R. Saito; Intrinsic strength and failure behaviors of ultra-small single-walled carbon nanotubes; *Comput. Mater. Sci.* 114 (2016) 167–171.
- [12] P. Giannozzi, S. Baroni, N. Bonini, M. Calandra, R. Car, C. Cavazzoni, D. Ceresoli, G.L. Chiarotti, M. Cococcioni, I. Dabo, A.D. Corso, S.D. Gironcoli, S. Fabris, G. Fratesi, R. Gebauer, U. Gerstmann, C. Gougoussis, A. Kokalj, M. Lazzeri, L. Martin-Samos, N. Marzari, F. Mauri, R. Mazzarello, S. Paolini, A. Pasquarello, L. Paulatto, C. Sbraccia, S. Scandolo, G. Sclauzero, A.P. Seitsonen, A. Smogunov, P. Umari, R.M. Wentzcovitch; Quantum espresso: a modular and open-source software project for quantum simulations of materials; *J. Phys. Condens. Matter* 21 (2009) 395502.
- [13] P. Hohenberg, W. Kohn; Inhomogeneous electron gas; *Phys. Rev.* 136 (1964) B864.
- [14] W. Kohn, L.J. Sham; Self-consistent equations including exchange and correlation effects; *Phys. Rev.* 140 (1965) A1133.
- [15] A.M. Rappe, K.M. Rabe, E. Kaxiras, J.D. Joannopoulos; Optimized pseudopotentials; *Phys. Rev. B* 41 (1990) 1227.
- [16] We used the pseudopotentials from <http://www.quantum-espresso.org>.
- [17] J.P. Perdew, K. Burke, M. Ernzerhof; Generalized gradient approximation made simple; *Phys. Rev. Lett.* 77 (1996) 3865.
- [18] H.J. Monkhorst, J.D. Pack; Special points for brillouin-zone integrations; *Phys. Rev. B* 13 (1976) 5188.
- [19] T. Mirfakhrai, R. Krishna-Prasad, A. Nojeh, J.D.W. Madden; Electromechanical actuation of single-walled carbon nanotubes: an Ab initio study; *Nanotechnology* 19 (2008) 315706.
- [20] G. Sun, J. Kürti, M. Kertesz, R.H. Baughman; Dimensional changes as a function of charge injection in single-walled carbon nanotubes; *J. Am. Chem. Soc.* 124 (2002) 15076–15080.